# Supporting Information

## Vertical phase separation induced highly efficient and stable pseudo-bilayer photoanode in organic photoelectrochemical cells

Jaehyeong Kim,[†, a] Soonyong Lee,[†, b] Yeonjeong Lee,[a] Tack Ho Lee,[c] Jin Young Kim[a, d,*],
Han Young Woo[b,*]

[a] School of Energy and Chemical Engineering, Ulsan National Institute of Science and Technology (UNIST), Ulsan 44919, Republic of Korea.

[b] Department of Chemistry, Korea University, Seoul 02841, Republic of Korea.

[c] Graduate Department of Chemical Materials, Institute for Plastic Information and Energy Materials, Sustainable Utilization of Photovoltaic Energy Research Center, Pusan National University, Busan 46241, Republic of Korea.

[d] Graduate School of Carbon Neutrality, Ulsan National Institute of Science and Technology (UNIST), Ulsan 44919, Republic of Korea.

Corresponding authors: J.Y. Kim (jykim@unist.ac.kr), H. Y. Woo (hywoo@korea.ac.kr)

[†] These authors contributed equally to this work.

## General

$^1$H and $^{13}$C-NMR spectra were acquired using Bruker Advance III HD spectrometers operating at 500 MHz and 125 MHz, respectively. UV-vis absorption spectra were recorded on a JASCO V-730 spectrophotometer. Cyclic voltammetry (CV) was conducted with a VersaSTAT 3 at a scan rate of 0.05 V $s^{-1}$, using 0.1 M tetrabutylammonium tetrafluoroborate ($Bu_4NBF_4$) in acetonitrile as the electrolyte. Each sample was drop-cast onto a platinum working electrode and measured using a conventional three-electrode system, with a platinum wire as the counter electrode and an $Ag/Ag^+$ reference electrode. GIWAXS measurements were carried out at the Pohang Accelerator Laboratory (PLS-II 9A U-SAXS). For incident angle-dependent GIWAXS experiments, measurements were performed at the same position while varying the X-ray incidence angle between 0.04° and 0.24°. The surface morphology of the films was examined via atomic force microscopy (AFM) using a Dimension ICON (Bruker Nano Surface) in ScanAsyst mode. Samples were prepared under optimized conditions for PEC devices. The dielectric constant of the blend films was measured by impedance spectroscopy using parallel-plate capacitor devices (ITO/active layer/Al) over a frequency range of 100 kHz to 100 Hz.[1] The relative permittivity ($\varepsilon_r$) was calculated using the equation, $\varepsilon_r = Cd/\varepsilon_0 A$, where $C$ is the measured capacitance, $\varepsilon_0$ is the permittivity of a vacuum ($8.854 \times 10^{-12}$ F $m^{-1}$), $A$ is the device area, and $d$ is the thickness of the BHJ film.

## Miscibility Analysis

Contact angles were measured with a KRÜSS DSA100 contact angle analyzer, and the surface energy was determined by measuring the contact angles of two probe liquids (water and ethylene glycol) according to the Owens-Wendt method. The surface energy ($\gamma_{sample}^{total}$) was calculated using the following equation: [2, 3]

$$\gamma_{water\ or\ EG}\left(cos\theta_{water\ or\ EG}+1\right)=2\left(\gamma_{sample}^{d}\times\gamma_{water\ or\ EG}^{d}\right)^{1/2}+2\left(\gamma_{sample}^{p}\times\gamma_{water\ or\ EG}^{p}\right)^{1/2}$$

where ($\gamma_{sample}^{total}$) is the surface energy of the sample, consisting of dispersive ($\gamma_{sample}^{d}$) and polar ($\gamma_{sample}^{p}$) components: $\gamma_{sample}^{total}=\gamma_{sample}^{d}+\gamma_{sample}^{p}$. By measuring the contact angles of water and EG, the dispersive and polar components of the surface energy were calculated. The Flory-Huggins interaction parameter between the donor and acceptor ($\chi^{D-A}$) is determined using the following equation:

$$\chi^{D-A}=\left(\sqrt{\gamma_{D}^{total}}-\sqrt{\gamma_{A}^{total}}\right)^{2}$$

where $\gamma_{D}^{total}$ and $\gamma_{A}^{total}$ represent the surface energies of the donor and acceptor materials, respectively.

## Fabrication of organic photoanode.

ITO substrates were sequentially cleaned by ultrasonication in deionized (DI) water, acetone, and isopropyl alcohol for 10 minutes each, followed by overnight drying in an oven. After an additional 15-minute UV/ozone treatment, a ZnO precursor solution (500 mg of zinc acetate dihydrate dissolved in 10 mL of 2-methoxyethanol, with 140 μL of ethanolamine as a stabilizer) was spin-coated at 4000 rpm for 40 seconds and annealed in air at 150 °C for 30 minutes. PPDT2FBT:IDIC and PPDT2FBT:IDIC-DEG blend solutions (1:1 weight ratio, 20 mg $mL^{-1}$ in chloroform) were spin-coated onto the ZnO layer, and the films were then annealed at 100 °C for 10 minutes inside a nitrogen-filled glove box.

**Photoelectrochemical Characterization.**

Photoelectrochemical characterization of the organic photoanodes was conducted in an air cell (with a light window) using a three-electrode configuration: a Ag/AgCl reference electrode, a Pt counter electrode, and the organic photoanode as the working electrode. The electrolytes used were 0.1 M potassium phosphate buffer (pH 7) and 0.2 M ascorbic acid (AA) in 0.1 M potassium phosphate buffer (pH 3.7). Linear sweep voltammetry (LSV) measurements were recorded using a potentiostat (IviumStat) under AM 1.5G illumination at 100 mW $cm^{-2}$, provided by a Xenon lamp (Newport Corporation), calibrated with a silicon photodiode. Applied potentials versus the reference electrode were converted to the reversible hydrogen electrode (RHE) scale using the Nernst equation: $E_{\mathrm{RHE}}\ (\mathrm{V}) = E_{\mathrm{Ag/AgCl}}\ (\mathrm{V}) + 0.059 \times \mathrm{pH} + 0.197$. The active area of the organic photoanode was 0.066 $cm^2$. A Mott-Schottky (M-S) plot was recorded with PPDT2FBT:IDIC and PPDT2FBT:IDIC-DEG-coated ITO/ZnO substrates as the working electrode.

**Materials**

Solvents and reagents were purchased from Sigma-Aldrich, Tokyo Chemical Industry (TCI), and ThermoScientific. Monomers such as indacenodithiophene (IDT) and 1-(dicyanomethylene)-3-indanone (INCN) were sourced from Solarmer. All chemicals were used as received, without further purification. IDIC[4,5] and PPDT2FBT[6] were synthesized following previously reported procedures from the literature.

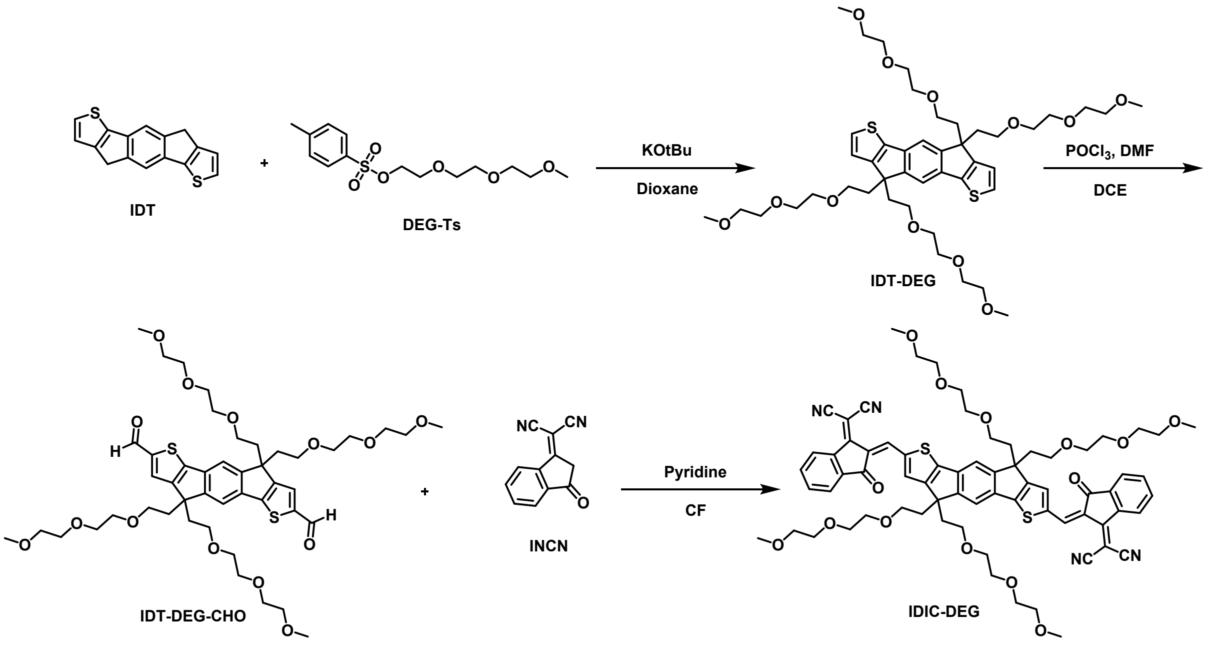

**Scheme S1**. Synthetic scheme of IDIC-DEG.

## Synthesis

### *(2-(2-(2-Methoxyethoxy)ethoxy)ethoxy)p-toluenesulfonate (DEG-Ts)*

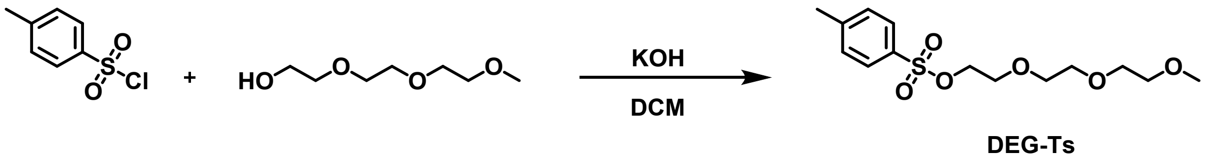

A mixture of triethylene glycol monomethyl ether (5 g, 30.4 mmol) and potassium hydroxide (12 g, 0.213 mol) was dissolved in 150 mL of dichloromethane (DCM). 4-Toluenesulfonyl chloride (7 g, 36.7 mmol) was then gradually added portion by portion while maintaining the temperature at 0 °C. Once the addition was complete, the reaction mixture was stirred at room temperature for 15 hours. The organic phase was extracted three times with DCM, dried over anhydrous magnesium sulfate. The resulting crude product, concentrated using rotary evaporation, was purified through silica gel column chromatography with ethyl acetate (EA) and hexane as the eluent = 1:2 (v/v). Yield: 10.7 g (92%). $^1$H NMR (500 MHz, CDCl$_3$): $\delta$ (ppm) 7.84 – 7.80 (m, 2H), 7.38 – 7.34 (m, 2H), 4.19 – 4.16 (m, 2H), 3.73 – 3.69 (m, 2H), 3.66 – 3.60 (m, 6H), 3.57 – 3.53 (m, 2H), 3.39 (s, 3H), 2.47 (s, 3H).

### *4,4,9,9-Tetrakis(2-(2-(2-methoxyethoxy)ethoxy)ethyl)-4,9-dihydro-s-indaceno[1,2-b:5,6 b']dithiophene (IDT-DEG)*

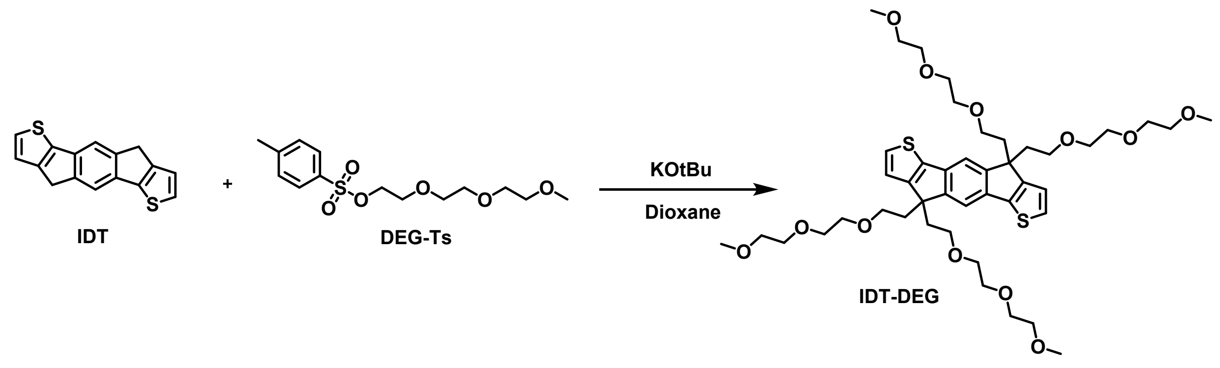

IDT (500 mg, 1.877 mmol) was dissolved in 25 mL of anhydrous dioxane, and potassium tert-butoxide (950 mg, 8.47 mmol) was gradually added in portions at 0 °C. The reaction mixture was stirred at room temperature for 2 hours before being cooled back to 0 °C. DEG-Ts (4.7 g, 15 mmol) was then added dropwise, and the mixture was stirred at 0 °C for 30 minutes, followed by stirring at room temperature for 1 hour. Subsequently, the temperature was increased to 40 °C, and the reaction continued for an additional 4 hours. Upon completion, the mixture was poured into ice water and filtered through a celite pad. The resulting filtrate was concentrated and purified via silica gel column chromatography using DCM and methanol (MeOH) as the eluent = 50:1 (v/v). Yield: 0.98 g (62%). $^1$H NMR (500 MHz, CDCl$_3$): $\delta$ (ppm) 7.36 (s, 2H), 7.31 (d, $J$ = 4.8 Hz, 2H), 7.03 (d, $J$ = 4.8 Hz, 2H), 3.58 (dd, $J$ = 5.7, 3.5 Hz, 8H), 3.53 – 3.48 (m, 16H), 3.36 (s, 12H), 3.34 – 3.29 (m, 8H), 2.94 (dq, $J$ = 13.1, 4.7 Hz, 8H), 2.43 (ddd, $J$ = 13.4, 9.3, 6.1 Hz, 4H), 2.31 (ddd, $J$ = 13.3, 9.3, 5.7 Hz, 4H). $^{13}$C NMR (125 MHz, $CDCl_3$): $\delta$ (ppm) 153.47, 151.98, 141.38, 135.32, 127.24, 121.68, 113.65, 71.89, 70.53, 70.49, 70.11, 67.38, 59.03, 49.67, 38.64.

*4,4,9,9-Tetrakis(2-(2-(2-methoxyethoxy)ethoxy)ethyl)-4,9-dihydro-s-indaceno[1,2-b:5,6-b']dithiophene-2,7-dicarbaldehyde (IDT-DEG-CHO)*

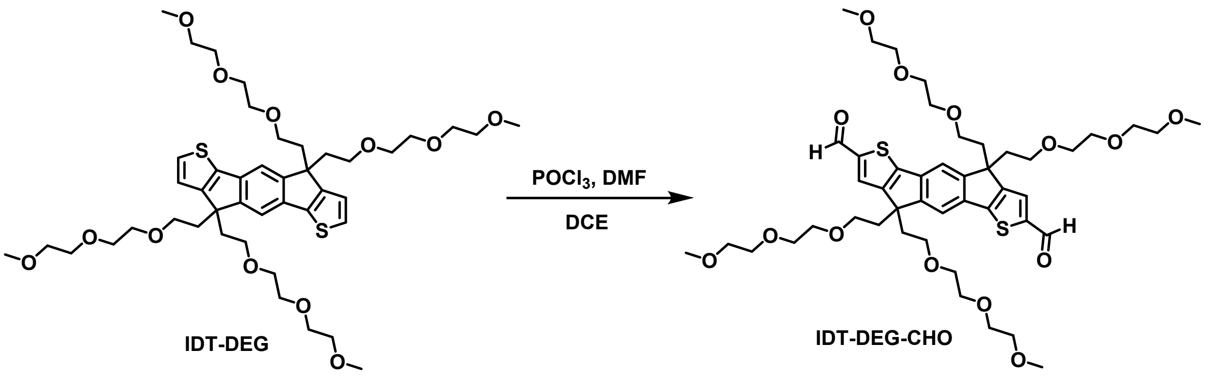

IDT-DEG (300 mg, 0.352 mmol) was dissolved in 10 mL of anhydrous dichloroethane (DCE) and 2 mL of anhydrous dimethylformamide (DMF). $POCl_3$ (3.8 g, 24.8 mmol) was gradually introduced dropwise at 0 °C, followed by stirring for an additional 2 hours. The reaction mixture was then heated to 70 °C and maintained under stirring for 12 hours. After cooling to 0 °C, 20 mL of a saturated sodium acetate solution was added, and the mixture was stirred at 70 °C for another 8 hours. Once the reaction was complete, the mixture was extracted with EA, dried over anhydrous sodium sulfate, and concentrated using a rotary evaporator. The resulting crude product was purified via silica gel column chromatography with EA and MeOH as the eluent = 50:1 (v/v). Yield: 0.145 g (45%). $^{1}$H NMR (500 MHz, $CDCl_3$): $\delta$ (ppm) 9.95 (s, 2H), 7.80 (s, 2H), 7.55 (s, 2H), 3.57 (dd, $J$ = 5.9, 3.2 Hz, 8H), 3.52 (dd, $J$ = 5.8, 3.3 Hz, 8H), 3.48 (t, $J$ = 4.7 Hz, 8H), 3.38 – 3.28 (m, 20H), 3.04 (dtd, $J$ = 27.1, 9.2, 5.8 Hz, 8H), 2.50 (ddd, $J$ = 14.1, 8.5, 5.9 Hz, 4H), 2.32 (ddd, $J$ = 13.9, 8.3, 5.7 Hz, 4H). $^{13}$C NMR (125 MHz, $CDCl_3$): $\delta$ (ppm) 183.17, 154.87, 154.19, 150.49, 145.99, 136.10, 131.54, 115.62, 71.87, 70.53, 70.51, 70.22, 67.30, 59.02, 50.57, 38.28.

*2,2'-((2Z,2'Z)-((4,4,9,9-tetrakis(2-(2-(2-methoxyethoxy)ethoxy)ethyl)-4,9-dihydro-s-indaceno[1,2-b:5,6-b']dithiophene-2,7-diyl)bis(methaneylylidene))bis(3-oxo-2,3-dihydro-1H-indene-2,1-diylidene))dimalononitrile* (*IDIC-DEG*)

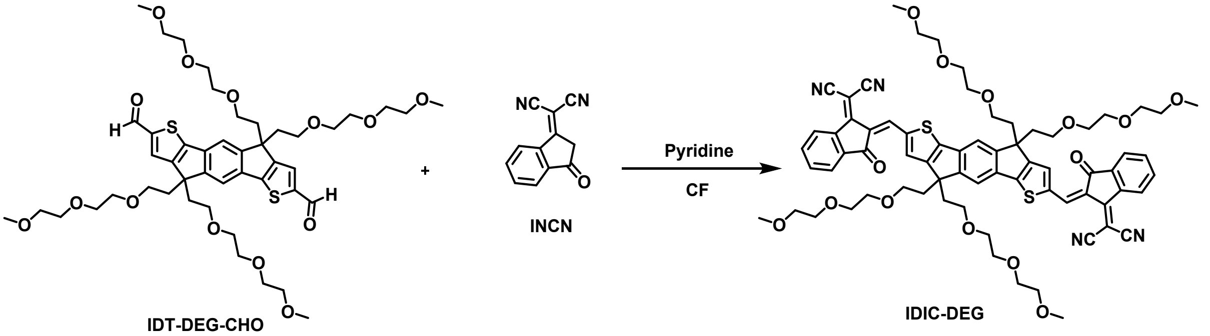

Under a nitrogen atmosphere, IDT-DEG-CHO (300 mg, 0.331 mmol) and INCN (194 mg, 1.00 mmol) were dissolved in 10 mL of anhydrous chloroform (CF). Anhydrous pyridine (925 mg, 11.55 mmol) was then added, and the mixture was refluxed for 20 hours. After the reaction was complete, the solution was directly concentrated, and the resulting crude product was purified via silica gel column chromatography using a CF and acetone mixture (5:1 v/v) as the eluent. Yield: 0.213 g (52%). $^1$H NMR (500 MHz, CDCl$_3$): $\delta$ (ppm) 8.96 (s, 2H), 8.72 (dd, $J$ = 7.0, 1.4 Hz, 2H), 7.96 (dd, $J$ = 6.6, 1.9 Hz, 2H), 7.85 (s, 2H), 7.78 (pd, $J$ = 7.3, 1.3 Hz, 4H), 7.66 (s, 2H), 3.54 (dd, $J$ = 5.8, 3.4 Hz, 8H), 3.50 – 3.43 (m, 16H), 3.37 – 3.28 (m, 20H), 3.14 – 3.02 (m, 8H), 2.49 (dt, $J$ = 14.0, 6.9 Hz, 4H), 2.32 (dt, $J$ = 13.9, 7.0 Hz, 4H). $^{13}$C NMR (125 MHz, CDCl$_3$): $\delta$ (ppm) 188.20, 160.53, 158.75, 156.06, 155.51, 141.18, 140.00, 138.38, 137.36, 136.98, 135.22, 134.55, 125.35, 123.87, 122.67, 116.43, 114.65, 114.60, 71.88, 70.51, 70.46, 70.29, 69.50, 67.32, 59.00, 50.58, 38.41.

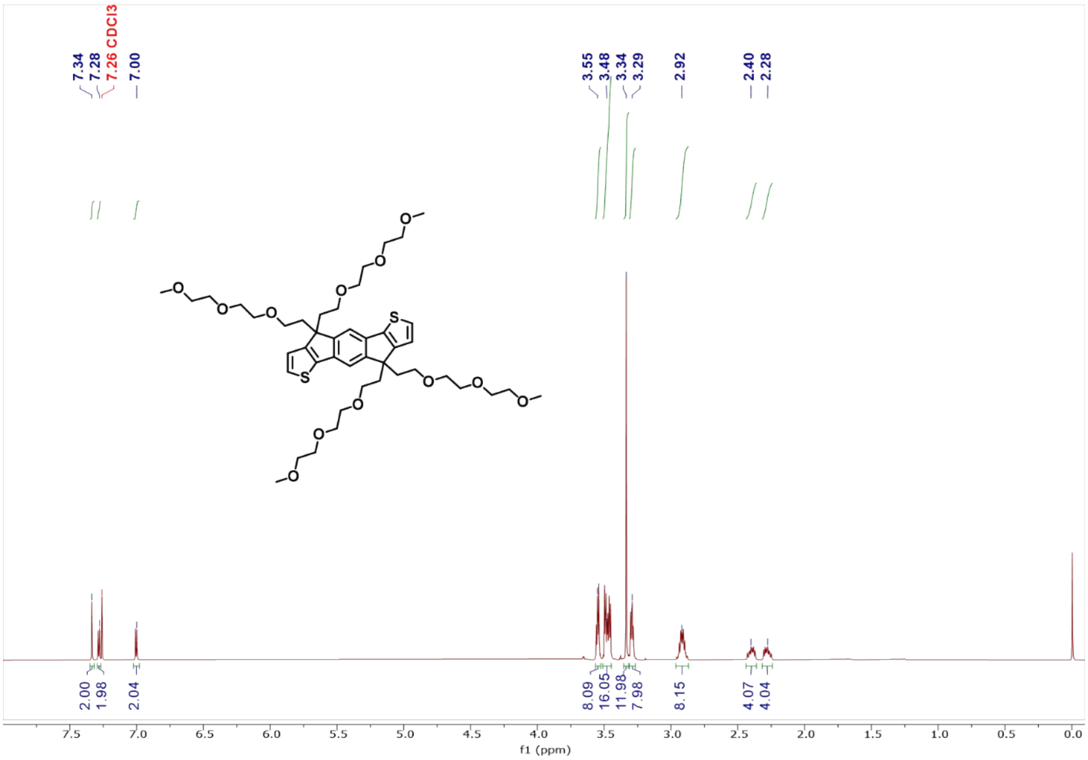

**Figure S1.** $^1$H-NMR spectrum of IDT-DEG in $CDCl_3$.

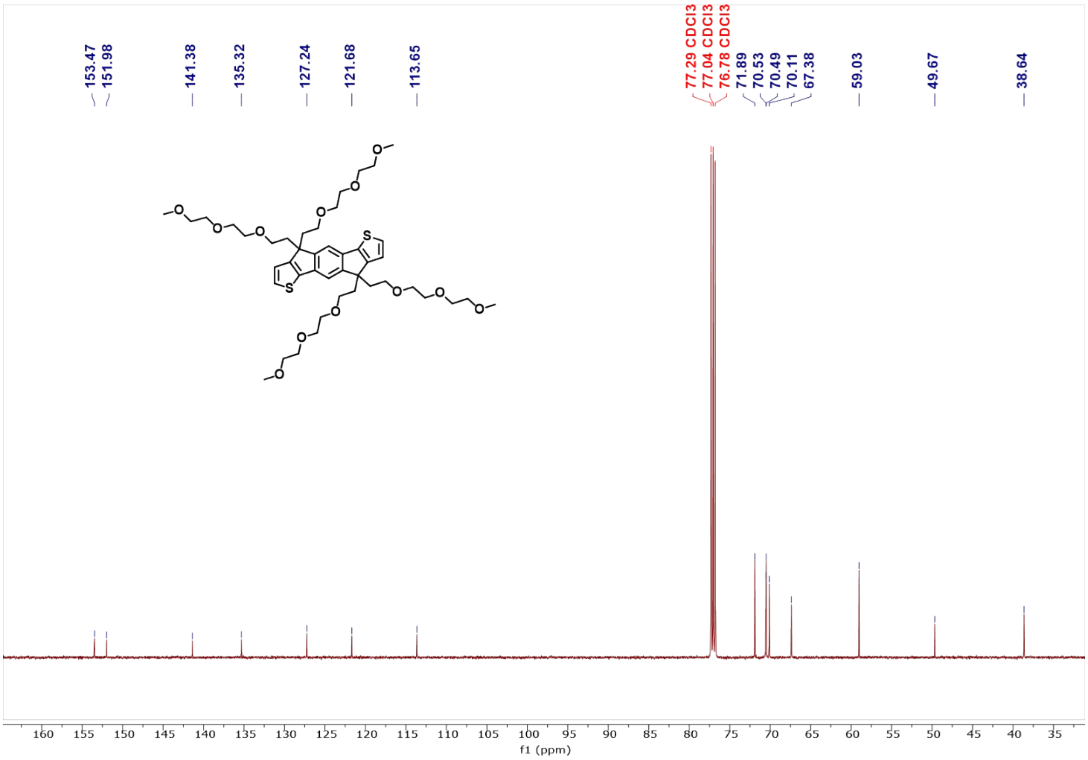

**Figure S2.** $^{13}$C-NMR spectrum of IDT-DEG in $CDCl_3$.

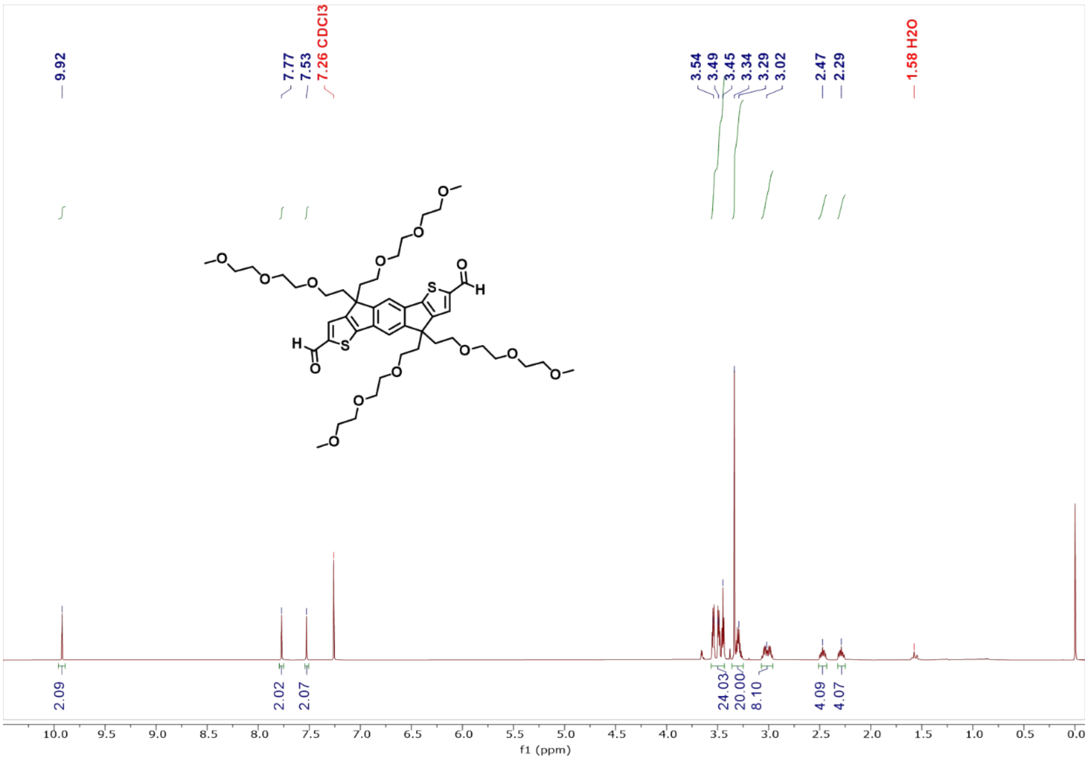

**Figure S3.** $^1$H-NMR spectrum of IDT-DEG-CHO in $CDCl_3$.

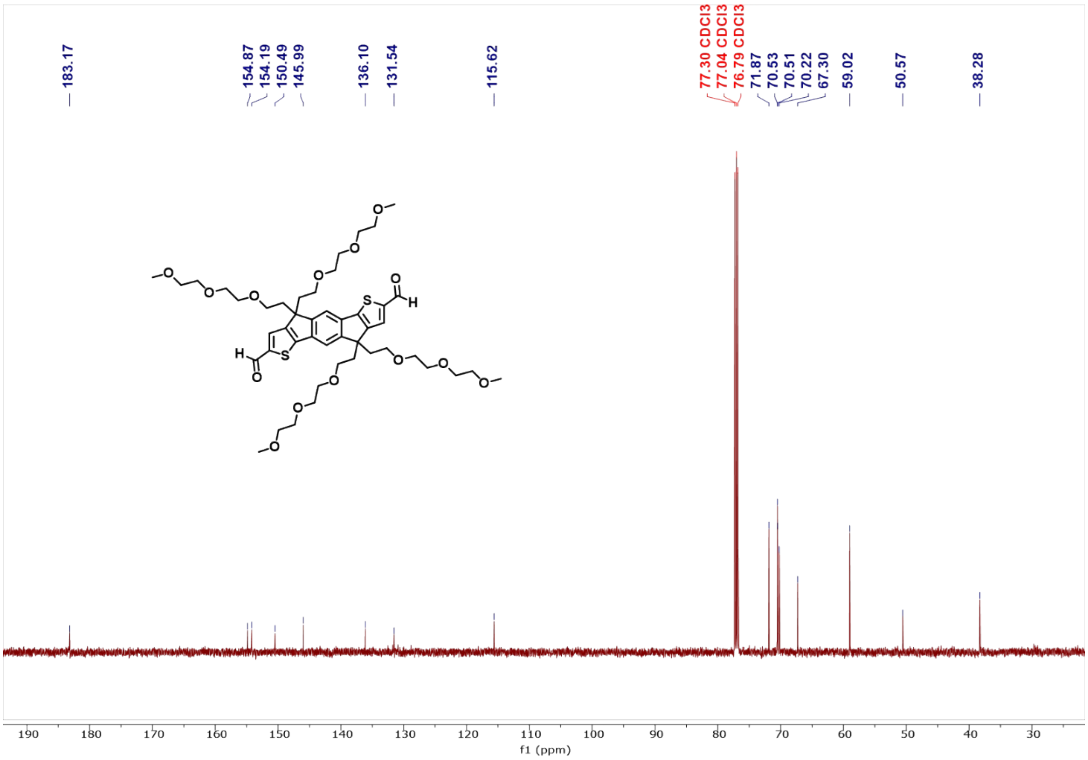

**Figure S4.** $^{13}$C-NMR spectrum of IDT-DEG in $CDCl_3$.

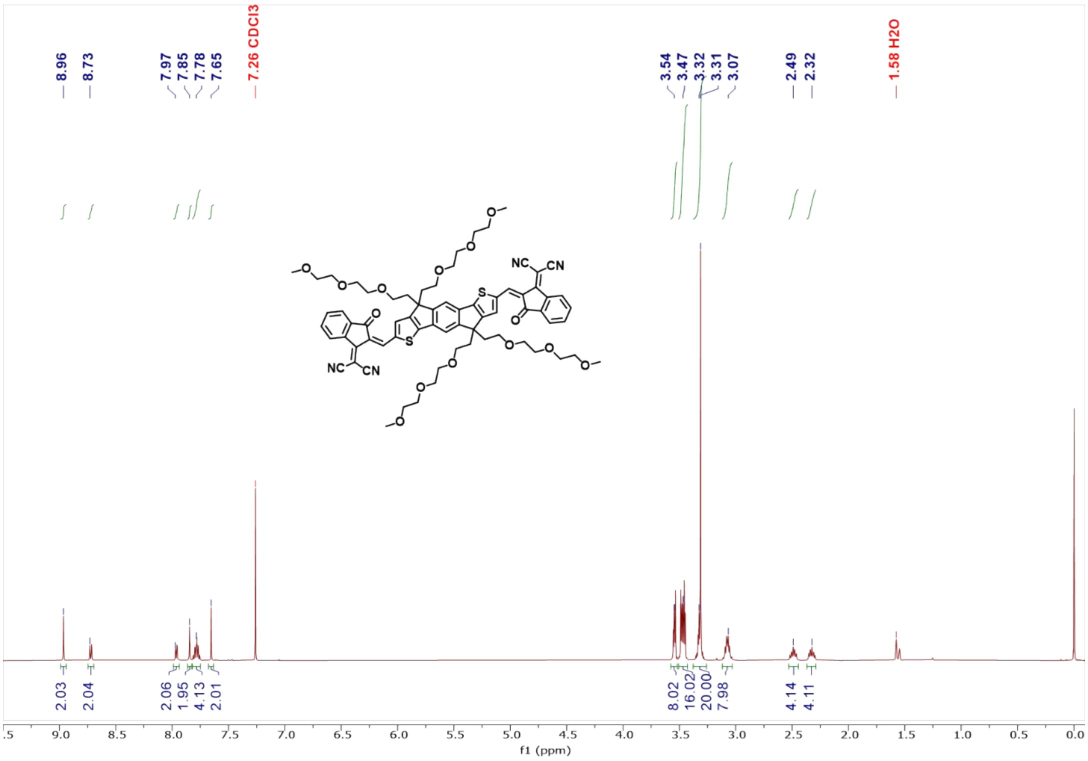

**Figure S5.** $^1$H-NMR spectrum of IDIC-DEG in $CDCl_3$.

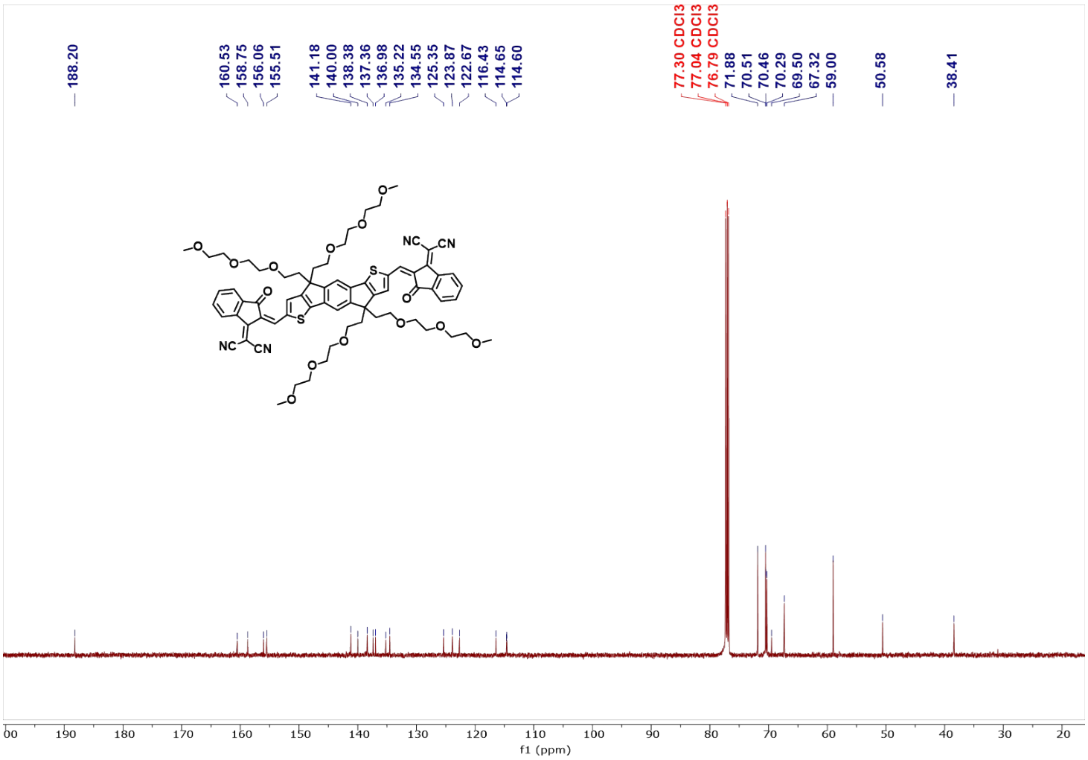

**Figure S6.** $^{13}$C-NMR spectrum of IDIC-DEG in CDCl$_3$.

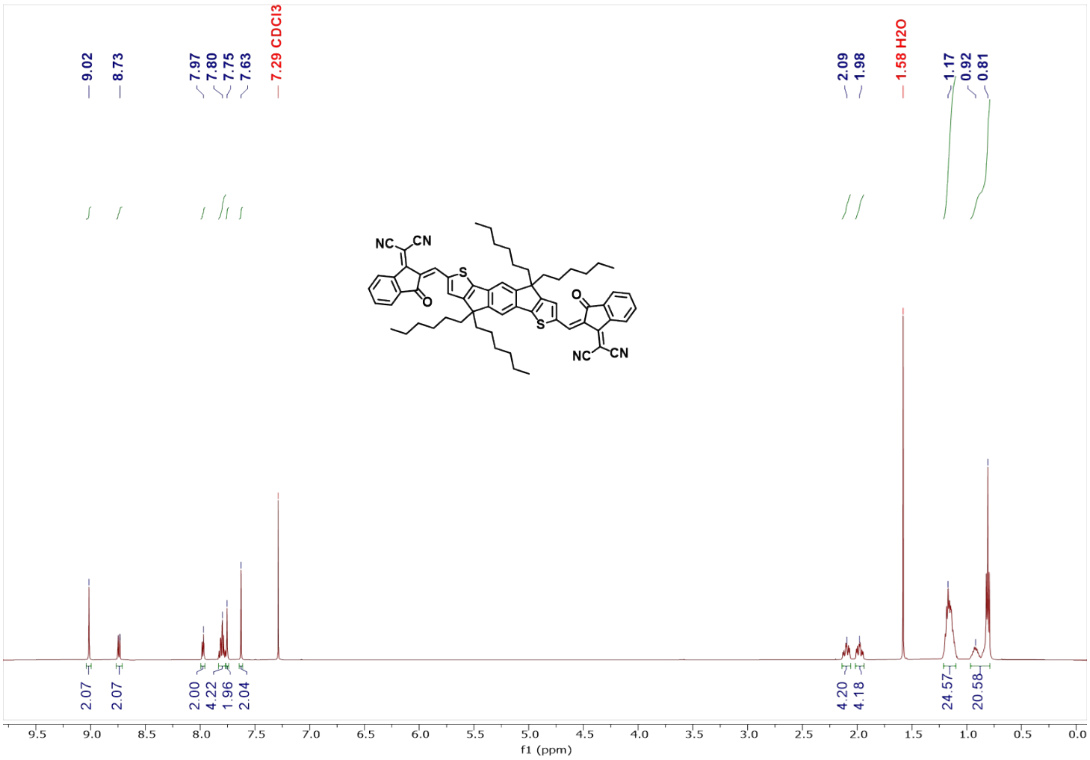

**Figure S7.** $^1$H-NMR spectrum of IDIC in $CDCl_3$.

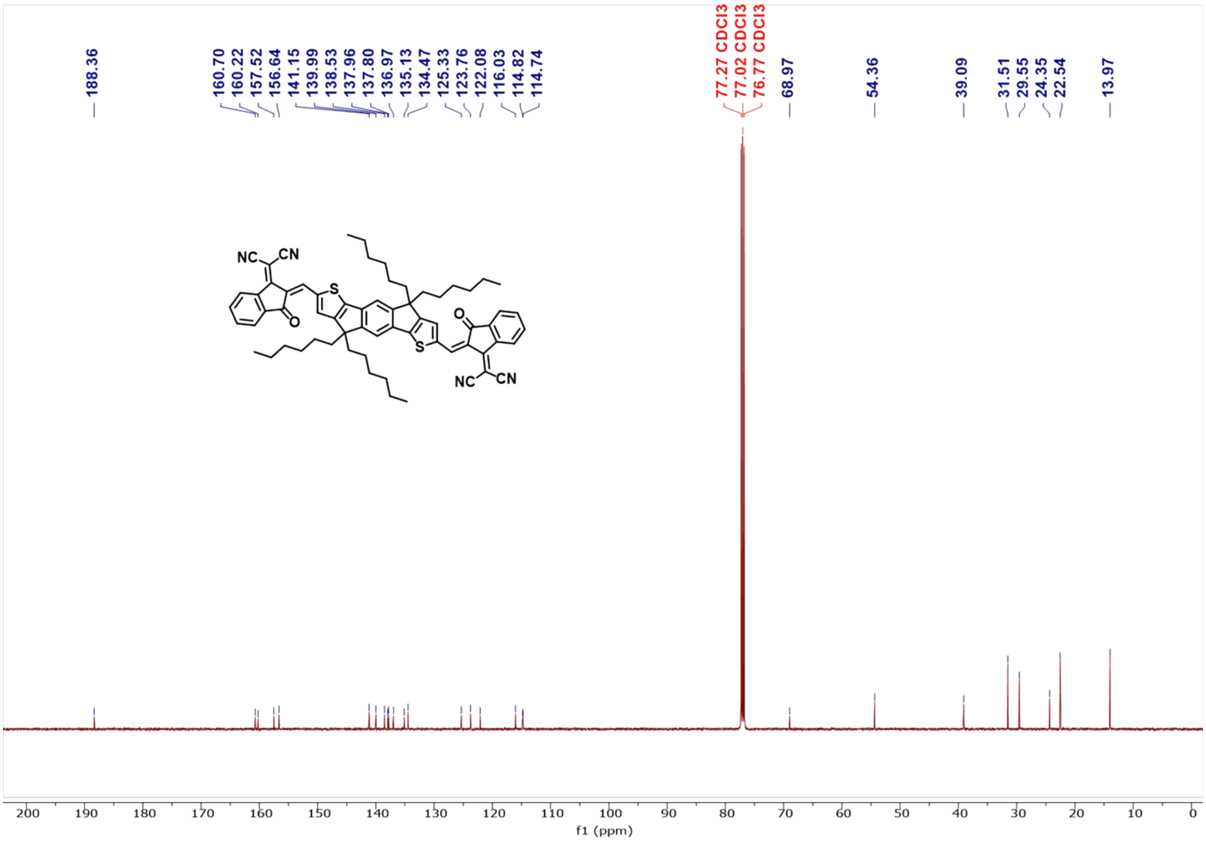

**Figure S8.** $^{13}$C-NMR spectrum of IDIC in CDCl$_3$.

**Poly[(2,5-bis(2-hexyldecyloxy)phenylene)-*alt*-(5,6-difluoro-4,7-di(thiophen-2-yl)benzo[*c*][1,2,5]-thiadiazole)] (PPDT2FBT) :** Yield: 62%. $M_n$ = 28 kDa, dispersity ($Đ$) = 2.2. $^1$H NMR (500 MHz, CDCl$_3$): $\delta$ (ppm) 8.32 (br, 2H), 4.09 (br, 2H), 2.14-0.72 (br, 62H).

**2,2′-((2Z,2′Z)-((4,4,9,9-tetrahexyl-4,9-dihydro-s-indaceno[1,2-b:5,6-b′]dithiophene-2,7-diyl)bis(methanylylidene))bis(3-oxo-2,3-dihydro-1H-indene-2,1-diylidene))dimalononitrile (IDIC)** : Yield: 64%. $^1$H NMR (500 MHz, CDCl$_3$): $\delta$ (ppm) 9.02 (s, 2H), 8.77 – 8.71 (m, 2H), 7.99 – 7.96 (m, 2H), 7.80 (pd, J = 7.3, 1.4 Hz, 4H), 7.75 (s, 2H), 7.63 (s, 2H), 2.10 (ddd, J = 13.5, 11.9, 4.7 Hz, 4H), 1.98 (ddd, J = 13.5, 11.8, 4.6 Hz, 4H), 1.21 – 1.10 (m, 25H), 0.97 – 0.79 (m, 21H). $^{13}$C NMR (125 MHz, CDCl$_3$): $\delta$ (ppm) 188.36, 160.70, 160.22, 157.52, 156.64, 141.15, 139.99, 138.53, 137.96, 137.80, 136.97, 135.13, 134.47, 125.33, 123.76, 122.08, 116.03, 114.82, 114.74, 68.97, 54.36, 39.09, 31.51, 29.55, 24.35, 22.54, 13.97.

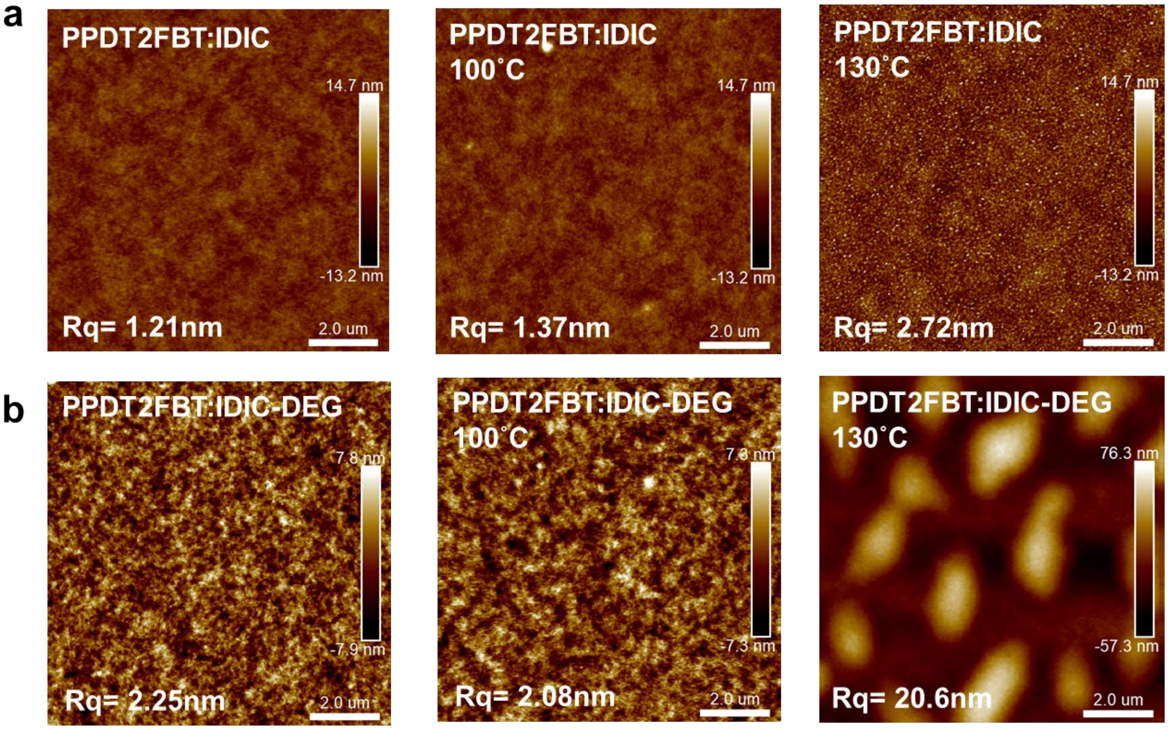

**Figure S9.** AFM height images of (a) PPDT2FBT:IDIC and (b) PPDT2FBT:IDIC-DEG films by changing thermal annealing temperatures.

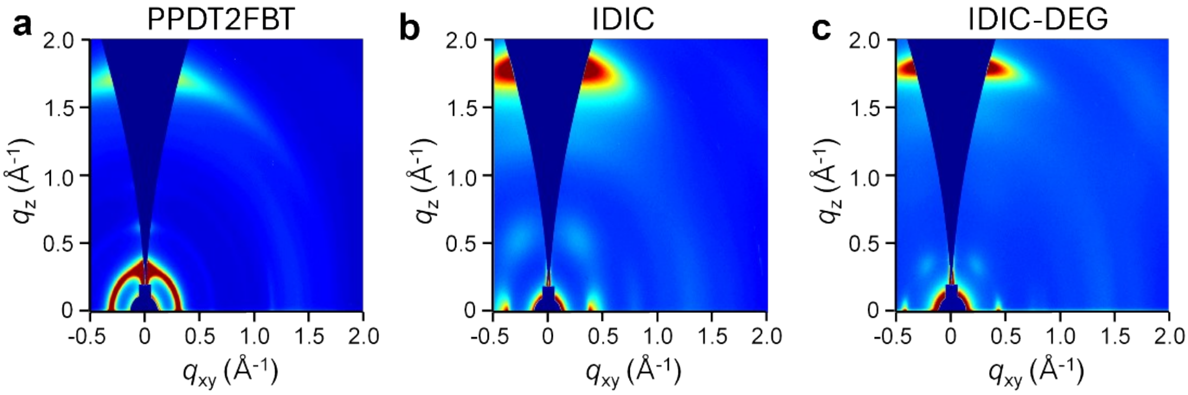

**Figure S10.** 2D GIWAXS images of (a) PPDT2FBT, (b) IDIC, and (c) IDIC-DEG films.

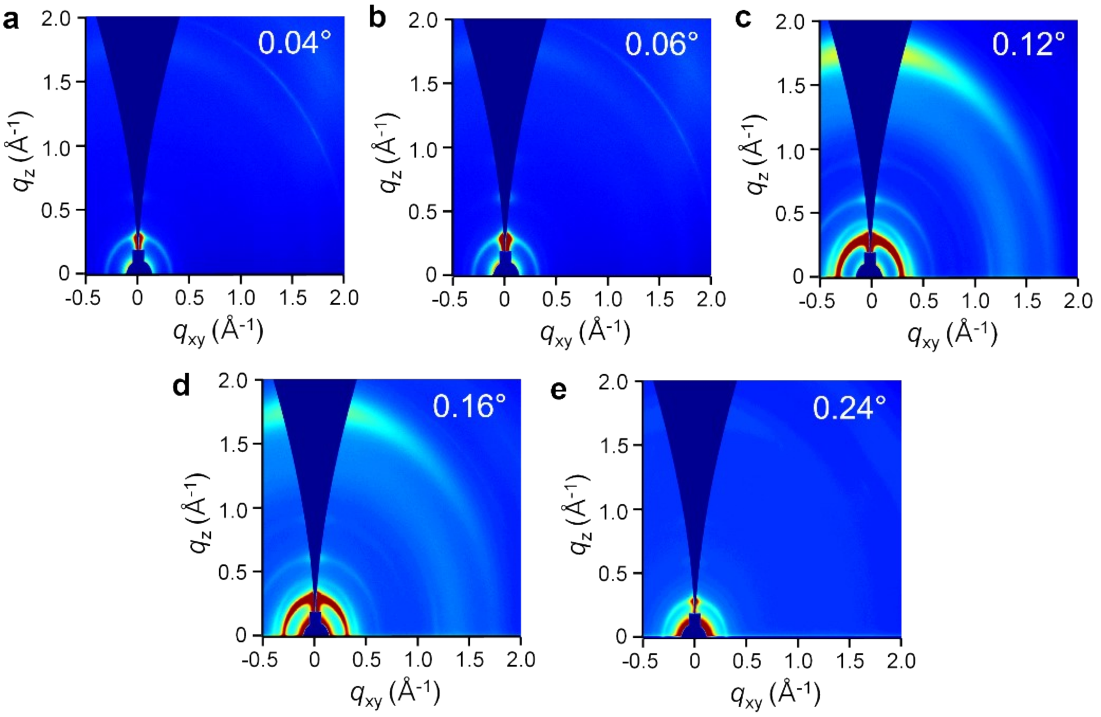

**Figure S11.** 2D GIWAXS images of PPDT2FBT:IDIC blend films at an incident angle of (a) 0.04°, (b) 0.06°, (c) 0.12°, (d) 0.16°, and (f) 0.24°. The films were annealed at 100 °C prior to measurement.

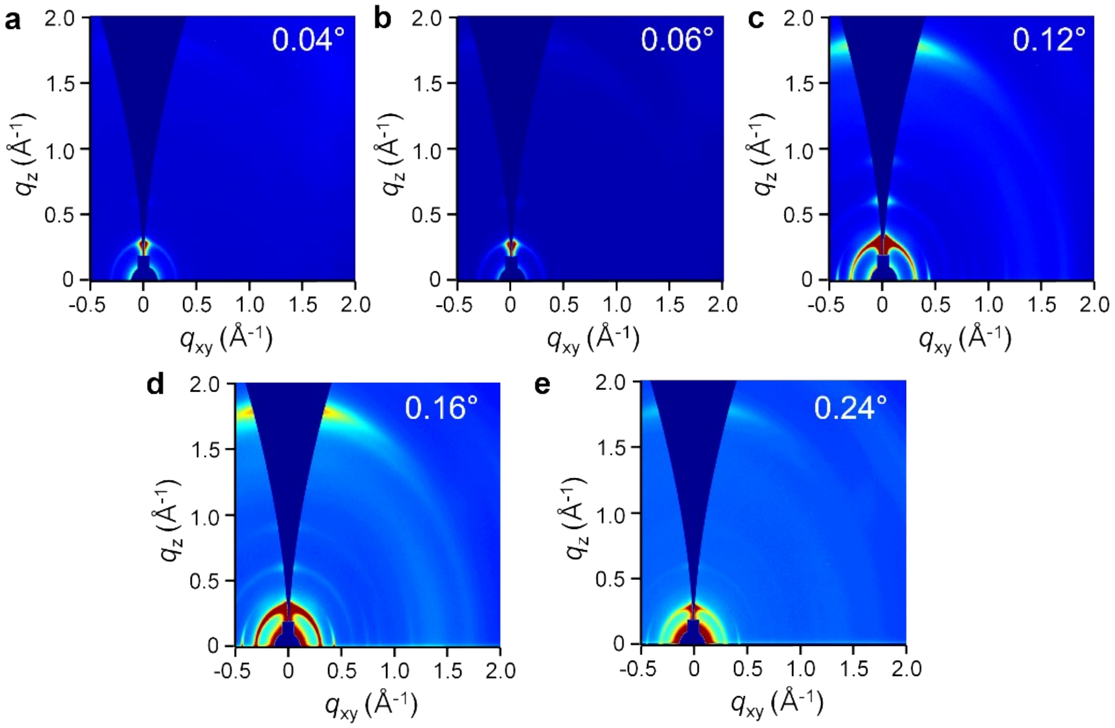

**Figure S12.** 2D GIWAXS images of PPDT2FBT:IDIC-DEG blend films at an incident angle of (a) 0.04°, (b) 0.06°, (c) 0.12°, (d) 0.16°, and (f) 0.24°. The film was annealed at 100 °C prior to measurement.

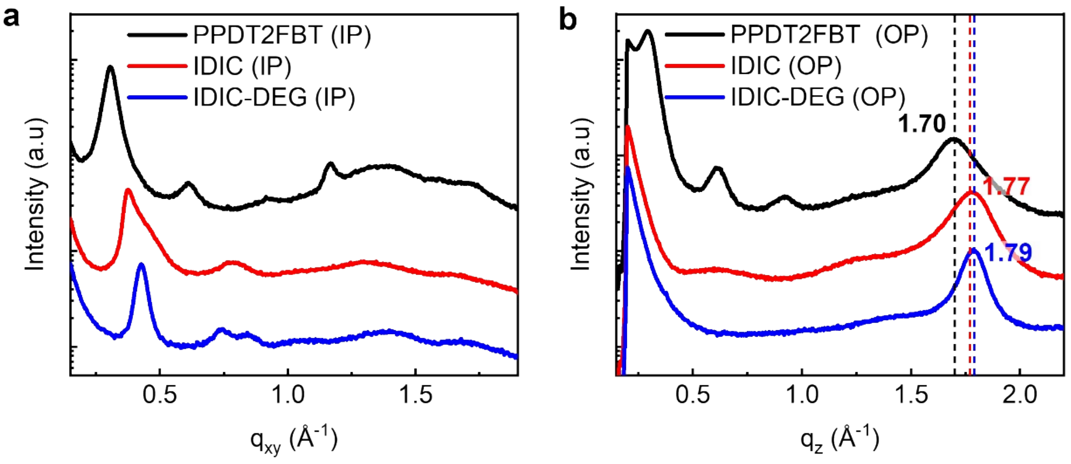

**Figure S13.** (a) In-plane and (b) out-of-plane GIWAXS line-cut profiles of PPDT2FBT, IDIC, and IDIC-DEG films.

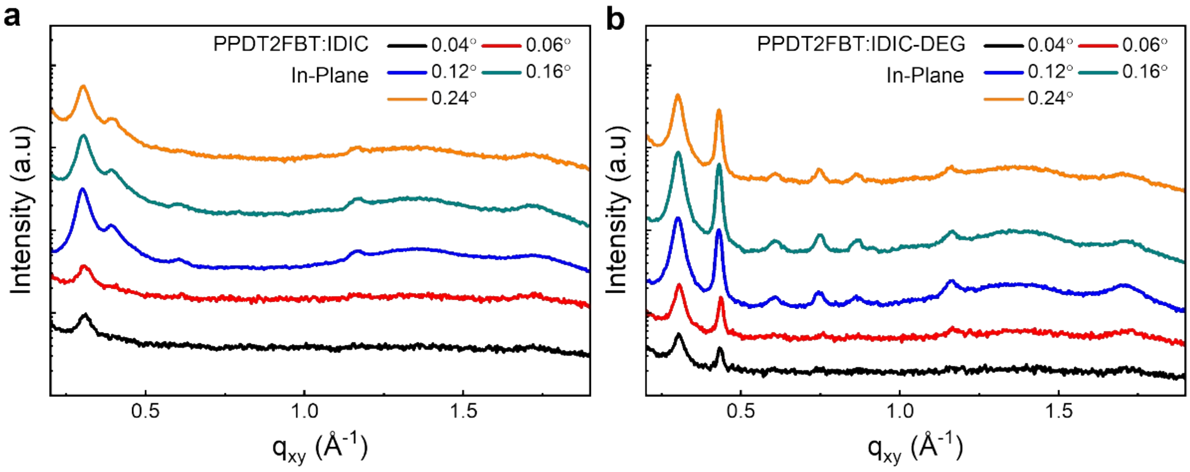

**Figure S14.** In-plane GIWAXS line-cut profiles (a) PPDT2FBT:IDIC and (b) PPDT2FBT:IDIC-DEG blend films at different incident angles.

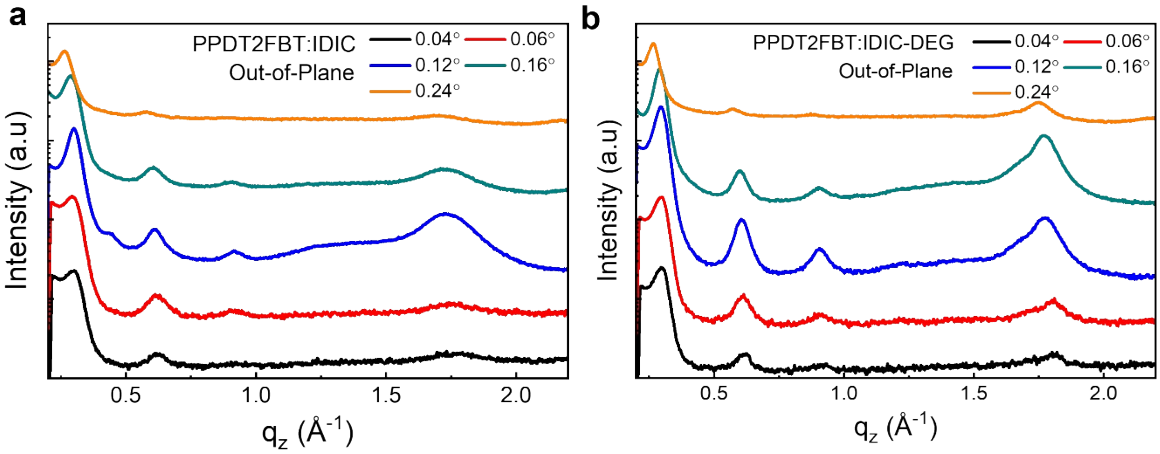

**Figure S15.** Out-of-plane GIWAXS line-cut profiles (a) PPDT2FBT:IDIC and (b) PPDT2FBT:IDIC-DEG blend films at different incident angles.

**Table S1.** Summary of GIWAXS packing parameters.

| Film | (100) Peak (IP) | | | | (010) Peak (OOP) | | | |
|---|---|---|---|---|---|---|---|---|
| | *q* (Å$^{-1}$) | d-spacing (Å) | FWHM (Å$^{-1}$) | CCL (Å) | *q* (Å$^{-1}$) | d-spacing (Å) | FWHM (Å$^{-1}$) | CCL (Å) |
| **PPDT2FBT** | 0.305 | 20.60 | 0.035 | 161.38 | 1.702 | 3.69 | 0.110 | 51.31 |
| **IDIC** | 0.378 | 16.62 | 0.068 | 53.16 | 1.773 | 3.54 | 0.118 | 47.88 |
| **IDIC-DEG** | 0.426 | 14.72 | 0.016 | 353.43 | 1.785 | 3.52 | 0.104 | 54.49 |

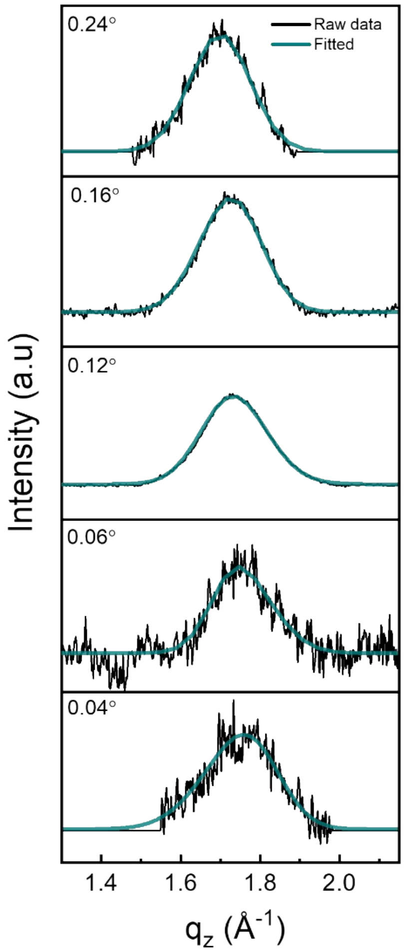

**Figure S16.** Out-of-plane (010) peak line-cut profiles of PPDT2FBT:IDIC blend films at different incident angles.

**Table S2.** Contact angle measurements and analysis of Flory-Huggins interaction parameters.

| | $\theta_{water}$ (deg) | $\theta_{EG}$ (deg) | $\gamma^{d}$ (mN m$^{-1}$) | $\gamma^{p}$ (mN m$^{-1}$) | $\gamma^{total}$ (mN m$^{-1}$) | $\chi^{D\text{-}A}$ |
|---|---|---|---|---|---|---|
| **PPDT2FBT** | 110.1 | 79.4 | 29.77 | 0.05 | 29.82 | - |
| **IDIC** | 92.1 | 61.9 | 30.06 | 1.76 | 31.82 | - |
| **IDIC-DEG** | 67.5 | 61.8 | 3.32 | 34.29 | 37.61 | - |
| **PPDT2FBT: IDIC** | 108.9 | 80.3 | 26.38 | 0.01 | 26.39 | 0.03 |
| **PPDT2FBT: IDIC-DEG** | 104.3 | 79.8 | 20.65 | 0.75 | 21.40 | 0.45 |
| **ITO** | 74.0 | 56.6 | 12.24 | 17.76 | 30.00 | - |
| **ZnO** | 40.4 | 38.5 | 2.07 | 64.62 | 66.68 | - |

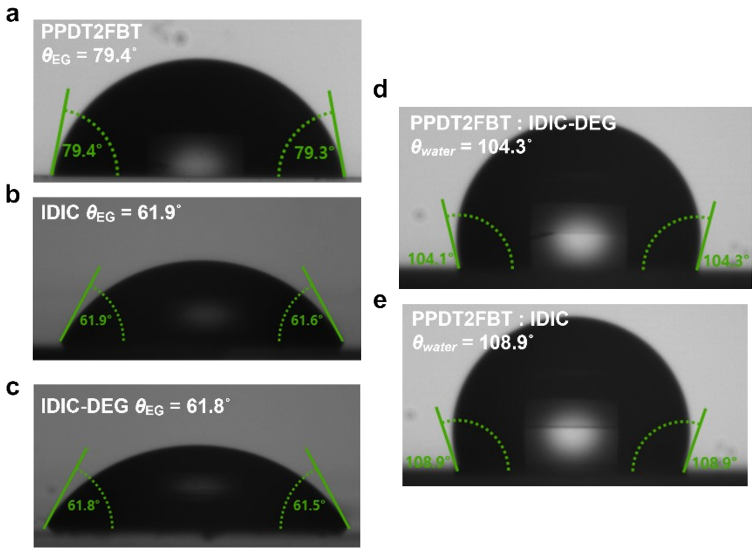

**Figure S17.** Contact angle measurements of ethylene glycol droplets on (a) PPDT2FBT, (b) IDIC, and (c) IDIC-DEG films. Water contact angle measurement of (d) PPDT2FBT:IDIC-DEG and (e) PPDT2FBT:IDIC blend films.

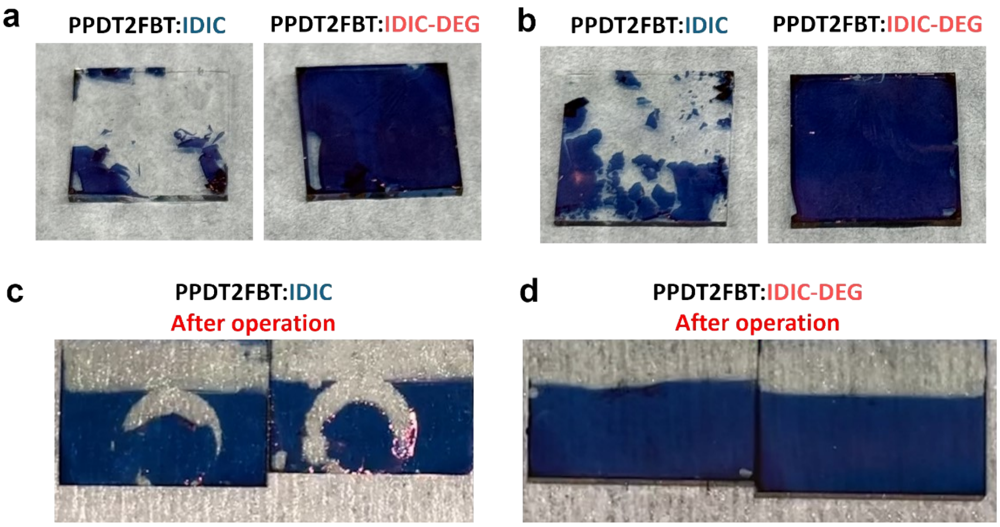

**Figure S18.** Photographic images of PPDT2FBT:IDIC and PPDT2FBT:IDIC-DEG films on (a) bare glass and (b) ITO/ZnO substrates after being immersed 12 hours in in 0.2 M ascorbic acid in 0.1 M potassium phosphate buffer solution (pH 3.7). Images of (c) PPDT2FBT:IDIC and (d) PPDT2FBT:IDIC-DEG films after PEC device operation.

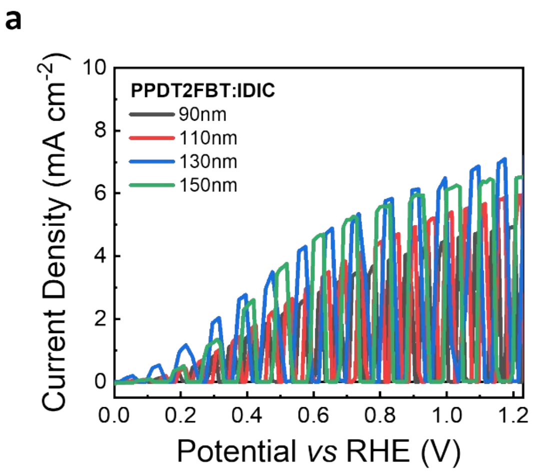

**Figure S19.** LSV scans of (a) PPDT2FBT:IDIC and (b) PPDT2FBT:IDIC-DEG photoanodes with different thickness of active layer in 0.1 M KPi buffer solution with 0.2 M AA under chopped 1 sun illumination.

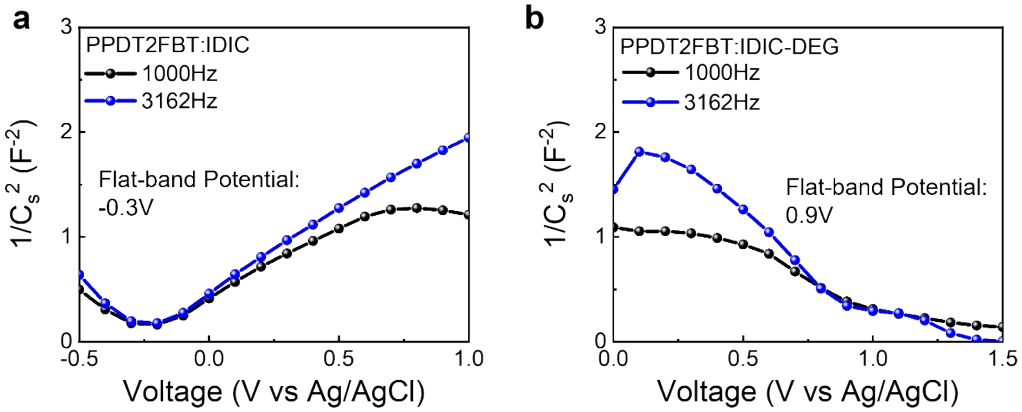

**Figure S20.** Mott-Schottky plots of (a) PPDT2FBT:IDIC and (b) PPDT2FBT:IDIC-DEG films were recorded in 0.1 M potassium phosphate buffer solution (pH 3.7), with an AC frequency of 1000 Hz and 3162 Hz, and an AC amplitude of 5 mV.

## Notes and references

1. S. Torabi, F. Jahani, I. Van Severen, C. Kanimozhi, S. Patil, R. W. Havenith, R. C. Chiechi, L. Lutsen, D. J. M. Vanderzande, T. J. Cleij, J. C. Hummelen and L. J. A. Koster *Adv. Funct. Mater.*, 2015, **25**, 150.
2. S. Pang, R. Zhang, C. Duan, S. Zhang, X. Gu, X. Liu, F. Huang and Y. Cao, *Adv. Energy Mater.,* 2019, **9**, 1901740.
3. X. He, C. C. S. Chan, X. Zou, S. Zhang, P. W. K. Fong, J. Kim, G. Li, X. Hu, W. Ma, K. S. Wong and W. C. H. Choy, *Adv. Energy Mater.*, 2023, **13**, 2203697.
4. L. Cai, T. Moehl, S.-J. Moon, J.-D. Decoppet, R. Humphry-Baker, Z. Xue, L. Bin, S. M. Zakeeruddin and M. Grätzel, *Org. Lett.*, 2014, **16**, 106-109.
5. Y. Lin, Q. He, F. Zhao, L. Huo, J. Mai, X. Lu, C.-J. Su, T. Li, J. Wang, J. Zhu, Y. Sun, C. Wang and X. Zhan, *J. Am. Chem. Soc.*, 2016, **138**, 2973-2976.
6. T. L. Nguyen, H. Choi, S.-J. Ko, M. A. Uddin, B. Walker, S. Yum, J.-E. Jeong, M. Yun, T. J. Shin, S. Hwang, J. Y. Kim and H. Y. Woo, *Energy Environ. Sci.*, 2014, **7**, 3040-3051